Phonon-Induced Anomalous Specific Heat of a Nanocrystalline Model Material by Computer Simulation

D. Wolf,[1,*] J. Wang,[1] S. R. Phillpot,[1] and H. Gleiter[2]
[1]*Materials Science Division, Argonne National Laboratory, Argonne, Illinois 60439*
[2]*Kernforschungszentrum Karlsruhe, Germany*
(Received 28 December 1994)

Atomistic simulations of the vibrational density of states of a space-filling nanocrystalline model material show low- and high-frequency tails not seen in the perfect crystal. The interface-related low-frequency phonon modes give rise to a pronounced, grain-size-dependent peak in the low-temperature excess specific heat that is also observed in glasses.

PACS numbers: 61.46.+w, 63.20.–e, 65.40.–f

The nature of grain boundaries (GBs) in nanocrystalline materials (NCMs) has been the subject of intense debate ever since the first ultrafine-grained polycrystals, with a typical grain size of 5–50 nm, were synthesized over a decade ago by consolidation of small clusters formed via gas condensation [1,2]. For some time it was thought that the atomic structures of the severely constrained GBs in NCMs differ fundamentally from those observed in coarse-grained or bicrystalline materials because, for a grain diameter of nanometer dimensions, a significant fraction of the atoms is situated in or near GBs and grain junctions [3,4]. The suggestion of a "frozen-gas-like" structure of the GBs [3,4] was aimed at explaining the rather unusual diffraction results; such a model might also explain some of the unusual—but controversial—thermal properties reported for NCMs, such as their enhanced specific heat [5,6] and lower Debye temperature [4,7]. However, recent experimental observations involving Raman spectroscopy [8], atomic-resolution transmission electron microscopy [9], and x-ray diffraction [10] indicate that the atomic structures of GBs in NCMs are, in fact, rather similar to those in coarse-grained polycrystalline or bicrystalline materials. Any attempt to elucidate the thermal properties of NCMs consequently requires, at the outset, a GB structural model that incorporates the severe microstructural constraints in NCMs and yet connects with the large body of knowledge on extended GBs in bicrystalline materials.

In this paper we present such a structural model tailored to capture what we consider the two essential structural features of NCMs, namely, microstructural constraints (i.e., a finite grain size) and the structural inhomogeneity due to the GBs and grain junctions, while still permitting the connection with bicrystalline GBs to be made. Using atomistic simulations, we determine how the low-temperature vibrational modes and the related thermal properties of this model NCM deviate from those of a perfect crystal and a glass. Our focus on the grain-size-dependent anomalous excess specific heat demonstrates that this extremely simple model, indeed, captures some of the essential structural features of NCMs and permits us to expose the lattice-vibrational origin of this anomaly and its intimate connection to the atomic-level disorder in the system.

The task of relating the structure and properties of the GBs in a polycrystal to those of corresponding bicrystalline GBs is extremely difficult as it requires three types of microstructural averages to be performed. These arise from the microstructural constraints present in a polycrystal and involve averages over (a) the five macroscopic degrees of freedom that each individual GB contributes to the total number of degrees of freedom of the polycrystal (three degrees associated with the misorientation between the grains and two characterizing the GB-plane normal [11]), (b) the various grain shapes, and (c) the distribution of grain sizes invariably present in polycrystals. In order to address, as directly as possible, the relationship between the highly constrained GBs in NCMs and the unconstrained GBs in bicrystals, the question we ask at the outset is this: As far as the total number of GB degrees of freedom, grain shapes, and grain sizes are concerned, what is the conceptually simplest polycrystal that one can, at least in principle, construct? In other words, what is the smallest number of geometrically distinct types of GBs, grain shapes, and grain sizes that a polycrystal has to contain and still be space filling?

Figure 1 shows that it is geometrically possible to construct a space-filling, three-dimensional polycrystal with a uniform (and unique) rhombohedral grain shape in which all GBs are crystallographically equivalent, i.e., a monodisperse polycrystal with exactly the same number of macroscopic degrees of freedom (at most 5) as the corresponding bicrystal, the only difference being the finite, variable grain size. Having thus eliminated the distributions in the types of GBs and grain shapes, our simulations of this model will focus entirely on the effect of the grain size (defined as the distance between the GBs), i.e., on the role of the microstructural constraints on the atomic structure and physical properties of a well-defined GB. Naturally, in the limit of infinite grain size, the model is designed to reproduce the related bicrystal structure.

The simulation cell in Fig. 1 contains two sets of distinct rhombohedral grains, each set delimited by six

 0031-9007/95/74(23)/4686(4)$06.00

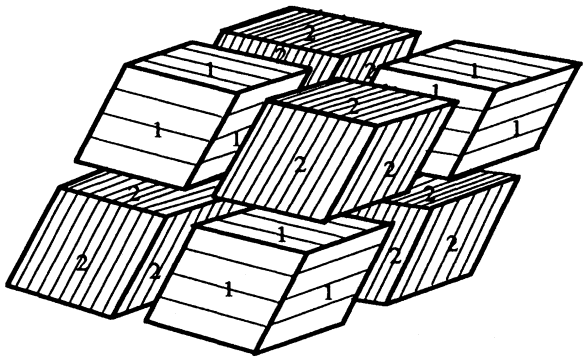

FIG. 1. Idealized space-filling polycrystal model. The three dimensionally periodic simulation cell shown here contains eight identically shaped rhombohedral grains delimited by two sets of crystallographically distinct surfaces (indicated by 1 or 2), forming a total of 24 crystallographically equivalent asymmetric tilt boundaries.

crystallographically equivalent surfaces, $\{hkl\}_1$ or $\{hkl\}_2$, respectively, and therefore forming 24 crystallographically equivalent asymmetric tilt boundaries (for details see Ref. [12]). We have constructed a series of four such model NCMs of increasing size (D = 8.2, 14.4, 20.6, and 26.9 Å, corresponding to 416, 2408, 7280, and 16 328 atoms in the simulation cell) in which one rhombohedron is bounded by {111} and the other by {115} planes, and all GBs are therefore asymmetric {115}{111} tilt boundaries. [The six faces of the {115} rhombohedra are thus delimited, for example, by the $(11\bar{5})$, $(1\bar{5}1)$, $(\bar{1}15)$, $(\bar{5}11)$, $(\bar{1}5\bar{1})$, and $(5\bar{1}\bar{1})$ planes and those of the {111} rhombohedra, for example, by the $(11\bar{1})$, $(1\bar{1}1)$, $(\bar{1}11)$, $(\bar{1}\bar{1}1)(\bar{1}1\bar{1})$, and $(1\bar{1}\bar{1})$ planes.] We hope to demonstrate below that this particular GB, with an energy of 674 ergs/cm^2 in the bicrystal, is reasonably representative of all the different types of boundaries that we could have chosen instead or additionally.

Lattice-statics simulations, in which the force on each atom and the external stresses on the simulation cell are iteratively reduced to zero by energy minimization, were used to determine the zero-temperature equilibrium structure of the NCMs. Since we are not interested in the properties of any specific material, the Lennard-Jones potential was used to describe the interatomic interactions. The energy and length scales in this potential (ε = 0.167 eV, σ = 2.315 Å) were fitted to the melting point T_m = 1356 K and zero-temperature lattice parameter a_0 = 3.616 Å of Cu with a cohesive energy E_{id} = −1.0378 eV/atom. Extensive comparisons with physically better justified many-body potentials have demonstrated that this simple potential represents face-centered-cubic (fcc) metals remarkably well [13]. This similarity is due to the fact that most interfacial phenomena are dominated by the short-range repulsions between the atoms (which are of a central-force type in both types of potentials).

The energy distribution function in Fig. 2 for the third-largest fully relaxed {115}{111} model NCMs shows three peaks, indicating three distinct types of crystal environments experienced by the atoms. The lowest-energy peak in Fig. 2, centered at E_{id}, corresponds to the grain interiors which, although slightly distorted and compressed, are essentially single crystalline. Detailed structural analysis shows the second peak to be due to the GBs, while the third peak arises from the grain junctions (i.e., the lines where four grain edges and the points where eight grain corners meet). As the grain size is reduced, the area under the perfect-crystal peak decreases until it disappears completely for the smallest grain size, indicating overlapping GBs; simultaneously, the areas under the two remaining peaks increase. Interestingly, the NCMs with the three largest grain diameters exhibit well-defined GBs with an atomic structure, energy, volume expansion, and width (of about $1.5a_0$) which differ remarkably little from those of the corresponding bicrystalline asymmetric {115}{111} tilt boundary [13].

The radial distribution function for the third-largest grain size is shown in Fig. 3, indicating excellent crystallinity of the material; similar plots were obtained even for the two smallest grain sizes. Corresponding to the reduced density (of 94.2% of that of the perfect crystal), the mean peak positions are shifted slightly to larger values with respect to the δ-function peaks in the perfect fcc crystal at T = 0 K (situated at $0.707a_0$, $1.0a_0$, $1225a_0$, etc).

The radial distribution function in Fig. 3 differs remarkably little from that obtained for the bicrystal (for the atoms within a distance of $\pm a_0$ from the GB; see also Ref. [14]). More importantly, the broadened peaks and the shift of the peak centers towards larger distances are generic features observed for virtually all GBs [13–15], suggesting that, as far as structural disorder is concerned,

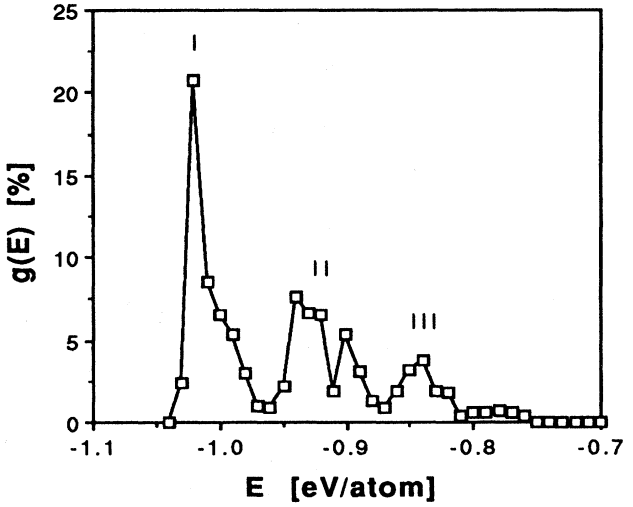

FIG. 2. Energy distribution function for the fully relaxed {115}{111} model NCM with a grain size of 20.6 Å.

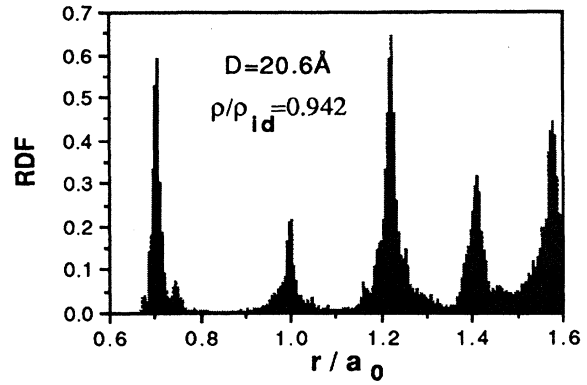

FIG. 3. Radial distribution function for the fully relaxed {115}{111} model NCM with a grain size of 20.6 Å.

the particular GB considered here is, indeed, reasonably representative.

Using the fully relaxed zero-temperature structures as starting points, lattice-dynamics simulations were performed to determine the phonon spectrum $g(\nu)$ (where ν is the phonon frequency), from which the low-temperature thermodynamic properties of the material, including the specific heat, can be determined [16]. Figure 4 compares the phonon density of states for the smallest {115}{111} model NCM (containing 416 atoms) with the phonon spectrum of a perfect (500-atom) fcc crystal and the 500-atom Lennard-Jones glass. Notice that, in agreement with recent Raman [17] and neutron-scattering [18] experiments, the density of states of the NCM exhibits modes at low and high frequencies not present in the perfect crystal. A detailed analysis of the eigenvectors associated with these modes shows that most are localized at the GBs and grain junctions, although there are also modes associated with collective vibrations of entire grains against each other [12].

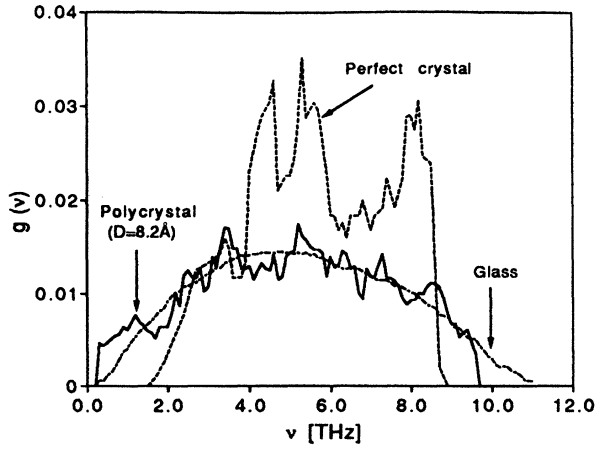

FIG. 4. Comparison of the vibrational density of states $g(\nu)$ for the {115}{111} model NCM with $D = 8.2$ Å (solid line) with those for a Lennard-Jones glass produced by molecular-dynamics simulation of a 500-atom quenched liquid (dash-dotted line) and for the perfect fcc crystal (dashed line); ν is the phonon frequency.

These low- and high-frequency modes originate from the broadening and shift in the peaks in the radial distribution function which are known to dominate also the anomalous elastic behavior of multilayered materials [14]. Distances shorter than in the perfect crystal give rise to elastic stiffening (or higher phonon frequencies), while larger distances and the overall volume expansion cause elastic (or phonon) softening [14,15]. The net elastic moduli of the system are, therefore, the result of a highly nonlinear averaging process over these competing contributions [14]; by contrast, the density of states shows both contributions explicitly. Based on this interpretation, one can expect a similar effect in the phonon spectrum of a glass (see Fig. 4) because the first and second peaks in the radial distribution function of a glass are similarly broadened (however, with washed-out higher peaks).

In the context of lattice dynamics it is well known that a finite system size gives rise to a sharp low-frequency (i.e., long-wavelength) cutoff in the density of states, by contrast with the well-established $g(\nu) \sim \nu^2$ variation for the lowest frequencies in a perfect crystal [16]. For example, on increasing the number of atoms in the perfect crystal from 108 to 500, we find that the smallest frequency in $g(\nu)$ decreases from 2.71 to 1.64 THz (see Fig. 4), while the maximum frequency is unaffected. By increasing the system size, this low-frequency cutoff can be shifted to ever lower frequencies and the ν^2 dependence can be obtained [19].

Interestingly, the specific heats obtained for the 108- and 500-atom perfect crystals are virtually indistinguishable, despite significantly differing phonon spectra for the lowest frequencies [12]. Moreover, the specific heat of the 500-atom perfect crystal exhibits good T^3 behavior, with a Debye temperature of 377 K [12] as compared with the experimental value of 316 K [20]. These observations demonstrate that the specific heat can be obtained reliably from even a relatively poor low-frequency approximation to the density of states [16].

Using the densities of states in Fig. 4, the specific heats of the four model NCMs and the glass may also be determined. Figure 5 shows the related specific heats in excess of that of the perfect crystal thus obtained. The excess specific heats of the NCMs exhibit pronounced, strongly grain-size dependent peaks at ~50 K (or ~4%–5% of the melting temperature). These peaks arise from those phonon modes that were shifted to low frequencies (see Fig. 4), as confirmed by the gradual disappearance of the anomaly when the lowest-frequency modes are progressively excluded from the NCM or glass spectra; by contrast, the omission of the shifted high-frequency modes has no effect [12].

The appearance of a pronounced low-temperature peak in the specific heat, with a height that decreases with increasing grain size, is in qualitative agreement with the experimental results [5,6]. It has been suggested that these

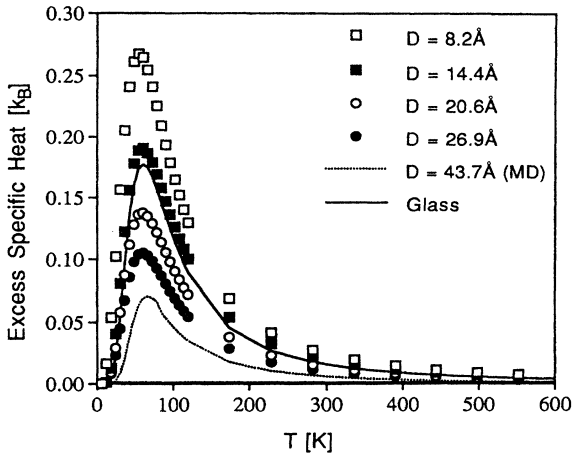

FIG. 5. Comparison of the temperature and grain-size dependence of the excess specific heat (in units of Boltzmann's constant, k_B) for the idealized {115}{111} model NCMs with that obtained for the Lennard-Jones glass (solid line) and for a nanocrystalline material with randomly oriented GBs and a grain size of 43.7 Å (dotted line). The latter was grown, via molecular-dynamics simulation, from the melt into which randomly oriented seeds were inserted [21].

anomalies may be due either to increased anharmonicity at the GBs or to the presence of light-element impurities [5]. While we cannot rule out any additional effects due to impurities, the existence of a similar anomaly in the glass demonstrates its origin in the low-frequency phonon modes due to the atomic-level disorder.

As one can expect for a system containing surfaces or interfaces [16], Debye's T^3 law for the specific heat is not obeyed in our model NCMs. If one were to, nevertheless, extract an effective Debye temperature, in qualitative agreement with the Mössbauer experiments [7], a substantially reduced effective value would be obtained.

The similarity of the specific-heat anomalies of the NCM and the glass and their common origin in the structural disorder in the material as seen in the radial distribution function suggest that the {115}{111} GB considered here exhibits a behavior that is reasonably representative of grain boundaries in general. To test this assertion, we have used molecular-dynamics simulations to crystallize from the melt a fully dense, three-dimensional NCM with random grain orientations and an average grain size of 43.7 Å [21]. Detailed structural characterization at zero temperature gives a system-averaged theoretical density of 97.5% and a radial distribution function very similar to that in Fig. 3; most of the GBs were identified as general GBs, with an average energy of about 730 ergs/cm^2. Subsequent lattice-dynamics simulations give the specific-heat anomaly shown in Fig. 5 (dotted line), with a maximum at virtually the same temperature as in the four model NCMs and in the glass, however, with a diminished peak height in accordance with the larger grain size.

In conclusion, in spite of its conceptual simplicity, the highly idealized model of a nanocrystalline material presented here combines the severe microstructural constraints associated with a small grain size with a realistic treatment of the GBs and provides insights not readily obtained from experiments. Most notably, the model demonstrates the existence of a specific-heat anomaly in nanocrystalline materials and states originating from the low-frequency phonon modes associated with the structural disorder in these metastable phases.

We have benefited from discussions with J. Eastman. This work was supported by the U.S. Department of Energy, BES Materials Sciences, under Contract W-31-109-Eng-38. We are grateful for additional support from the Deutsche Forschungsgemeinschaft (Leibniz program) and the A. v. Humboldt and Max-Planck Foundations (Max-Planck Research Award program).

*Electronic address: Dieter_Wolf@QMGATE.ANL.GOV

[1] H. Gleiter, in *Proceedings of the Second Risø International Symposium on Metallugry and Materials Science,* edited by N. Hansen *et al.* (Roskilde, Denmark, 1981).
[2] R. Birringer *et al.,* Phys. Lett. **102A**, 365 (1984).
[3] X. Zhu *et al.,* Phys. Rev. B **35**, 9085 (1987).
[4] H. Gleiter, Prog. Mater. Sci. **33**, 223 (1989).
[5] J. Rupp and R. Birringer, Phys. Rev. B **36**, 7888 (1987); A. Tschöpe and R. Birringer, Acta Metall. Mater. **41**, 2791 (1993); Philos. Mag. B **68**, 2223 (1993).
[6] H. G. Klein, Diplom thesis, Universität des Saarlandes, 1992 (unpublished).
[7] J. Jiang *et al.,* Solid State Commun. **80**, 525 (1991).
[8] C. A. Melendres *et al.,* J. Mater. Res. **4**, 1246 (1989).
[9] G. J. Thomas *et al.,* Scripta Metall. **24**, 201 (1990).
[10] J. Eastman *et al.,* Philos. Mag. B **66**, 667 (1992).
[11] See, for example, D. Wolf, in *Materials Interfaces: Atomic-Level Structure and Properties,* edited by D. Wolf and S. Yip (Chapman and Hall, London, 1992), p. 16.
[12] J. Wang, D. Wolf, S. R. Phillpot, and H. Gleiter, Philos. Mag. A (to be published).
[13] See, for example, D. Wolf and K. L. Merkle, in Ref. [11], p. 87.
[14] D. Wolf and J. Lutsko, Phys. Rev. Lett. **60**, 1170 (1988).
[15] D. Wolf and J. Jaszczak, J. Comp.-Aided Mat. Design **1**, 111 (1993).
[16] A. A. Maradudin *et al.,* in *Solid State Physics,* edited by H. Ehrenreich *et al.* (Academic Press, New York, 1971), Suppl. 3.
[17] E. D. Obraztsova *et al.,* in Proceedings of the 2nd International Conference on Nanostructured Materials, Stuttgart, 1994 [Nanocryst. Matls. (to be published)].
[18] J. Trampeneau *et al.,* in Ref. [17].
[19] V. Rosato *et al.,* Philos. Mag. A **59**, 321 (1989).
[20] J. de Launay, in *Solid State Physics,* edited by F. Seitz and D. Turnbull (Academic Press, New York, 1956), Vol. 2.
[21] S. R. Phillpot, D. Wolf, and H. Gleiter, J. Appl. Phys. (to be published).